LOW FREQUENCY SCATTERING *

by

T. B. A. Senior
The Radiation Laboratory
The University of Michigan
Ann Arbor, Michigan 48105

Abstract

The leading terms in the low frequency expansions for acoustically soft and hard bodies are examined and the relevance of the magnetic polarizability tensor is discussed. For a hard, rotationally symmetric body, two tensor elements, functions only of the geometry, are now sufficient to specify the entire low frequency scattering behavior in just the same way as the electrostatic capacity suffices for a soft body. Even these quantities are subject to known constraints and computed data for a variety of bodies are presented.

---

* This work was supported by the Air Force Office of Scientific Research under Grant 72-2262.

Introduction

When a body is illuminated by an acoustic plane wave whose wave number k is sufficiently small, the scattered field at large distances can be expanded in a series of increasing positive powers of k. If the body is soft, it is well known that the leading term is $O(k^0)$ and proportional to the electrostatic capacity, which can be found by solving a potential problem for the geometry in question. For a hard body, on the other hand, the leading term is proportional to k^2 and is a function of the directions of incidence and scattering, but these dependences can be separated out by introducing the concept of the magnetic polarizability tensor $\overline{\overline{M}}$. This is related to the virtual mass tensor $\overline{\overline{W}}$ and, like the capacity, is a function only of the geometry of the body.

For a rotationally symmetric shape, the tensor $\overline{\overline{M}}$ naturally diagonalises and just two of its elements are independent. These are sufficient to specify the low frequency scattering from a hard body for any directions of incidence and observation, and play the same role as the electrostatic capacity, C/ϵ, in scattering from a soft body. Like the capacity, the elements M_{11} and M_{33} are subject to known constraints in terms of the geometry, and these can serve to establish bounds on the scattering. Moreover, for a variety of bodies, the variations in M_{11}, M_{33} and C/ϵ can be reduced by appropriate normalisation. This is illustrated using exact data computed for prolate and oblate spheroids, lenses and ogives, finite cones of acute and obtuse angles, and right-circular and capped cylinders. It would now appear that for many practical purposes sufficient accuracy can be achieved using, for example, the spheroid as a model.

1. ANALYSIS

Consider a finite, closed acoustically soft or hard body B illuminated by a plane acoustic wave having velocity potential[1]

$$U^i = e^{ik\hat{k}\cdot\underline{r}} \tag{1}$$

where $\underline{r}$ is the radius vector to an arbitrary point in the domain $\mathcal{V}$ exterior to B, $\hat{k}$ is a unit vector in the direction of propagation and k is the wave number. A time factor $e^{-i\omega t}$ is assumed and suppressed. For k sufficiently small, $U^i(\underline{r})$ at points in the vicinity of B can be expanded as

$$U^i(\underline{r}) = \sum_{m=0}^{\infty} (ik)^m U_m^i(\underline{r}) \ , \tag{2}$$

and in particular,

$$U_o^i(\underline{r}) = 1 \ , \quad U_1^i(\underline{r}) = \hat{k}\cdot\underline{r} \ . \tag{3}$$

Since the scattered field $U^s(\underline{r})$ can be similarly expanded, so can the total field $U(\underline{r})$, viz.

$$U(\underline{r}) = \sum_{m=0}^{\infty} (ik)^m U_m(\underline{r}) \tag{4}$$

and $U_o(\underline{r})$ and $U_1(\underline{r})$ both satisfy Laplace's equation. The task is to find the leading term in the low frequency expansion of $U^s(r)$ at large distances from the body, and this requires the solution of the near field problem, followed by its continuation into the far zone.

Let us treat first the case in which B is a soft body for which the boundary condition is

$$U(\underline{r}) = 0 \ , \quad \underline{r} \text{ on } B \ . \tag{5}$$

When this is inserted into the Helmholtz representation for the field at a point $\underline{r}$ near B and the lowest order (in k) terms extracted, it is found that in the limit as $\underline{r}$ approaches B

$$\frac{1}{4\pi}\int_B \frac{1}{R}\frac{\partial}{\partial n'} U_o(\underline{r}')\, dS' = 1 \quad , \tag{6}$$

where $R = |\underline{r} - \underline{r}'|$ and n' is in the direction of the unit outward normal at $\underline{r}'$. The integral equation (6) is identical to the equation for the surface charge distribution on a metallic conductor raised to unit potential. Indeed, if ϵ is the permittivity of the surrounding medium, the surface charge density is

$$\rho = \epsilon \frac{\partial U_o}{\partial n} \tag{7}$$

and

$$\int_B \frac{\partial}{\partial n'} U_o(\underline{r}')\, dS' = \frac{C}{\epsilon} \tag{8}$$

where C is the electrostatic capacity.

In the far zone ($r \to \infty$), the Helmholtz representation leads to an expression for $U^s(\underline{r})$ as an integral over B, and when the boundary condition (5) is applied and the expansion (4) inserted, we have

$$U^s(\underline{r}) \sim \frac{e^{ikr}}{4\pi r}\left\{-\int_B \frac{\partial}{\partial n'} U_o(\underline{r}')\, dS' + ik\int_B \left[\hat{r}.\underline{r}' \frac{\partial}{\partial n'} U_o(\underline{r}') - \frac{\partial}{\partial n'} U_1(\underline{r}')\right] dS' + O(k^2)\right\}. \tag{9}$$

Hence

$$U^s(\underline{r}) \sim \frac{e^{ikr}}{r}\left\{-\frac{C}{4\pi\epsilon} + O(k)\right\}, \tag{10}$$

which is a well known result. Using reciprocity, Van Bladel[2] has also shown

that

$$\int_B \frac{\partial}{\partial n'} U_1(\underline{r}')\, dS' = \int_B \left(\hat{k}\cdot\underline{r}' - \frac{C}{4\pi\epsilon}\right) \frac{\partial}{\partial n'} U_o(\underline{r}')\, dS' \quad ,$$

so that a knowledge of $\frac{\partial U_o}{\partial n}$ is sufficient to specify two terms in the far zone:

$$U^s(\underline{r}) \sim \frac{e^{ikr}}{4\pi r}\left\{ -\frac{C}{\epsilon} + ik\left[\frac{1}{4\pi}\left(\frac{C}{\epsilon}\right)^2 + (\hat{r}-\hat{k})\cdot\int_B \underline{r}' \frac{\partial}{\partial n'} U_o(\underline{r}')\, dS'\right] + O(k^2)\right\} \qquad (11)$$

The integral term is absent in the forward scattering direction ($\hat{r}=\hat{k}$) and in addition the integral itself vanishes if the origin of coordinates is chosen at the center of gravity of the charge distribution — a location which is obvious for a symmetric body, but which in general can be found only when $\frac{\partial U_o}{\partial n}$ has been determined. In either case,

$$U^s(\underline{r}) \sim \frac{e^{ikr}}{4\pi r}\left(-\frac{C}{\epsilon}\right)\left\{1 - \frac{ik}{4\pi}\frac{C}{\epsilon} + O(k^2)\right\} , \qquad (12)$$

and the electrostatic capacity alone now specifies two terms in the expansion.

For the hard body the analysis is a little more involved. The boundary condition on $U(\underline{r})$ is

$$\frac{\partial}{\partial n} U(\underline{r}) = 0 \quad , \quad \underline{r} \text{ on } B \quad , \qquad (13)$$

leading to similar conditions on the partial fields $U_m(\underline{r})$, and from these it can be shown that $U_o^s(\underline{r})$ is zero everywhere, implying $U_o(\underline{r}) = 1$. For the field $U_1(\underline{r})$ an integral equation can be obtained in the same manner as for a soft body, and is

$$U_1(\underline{r}) = 2\hat{k}.\underline{r} + \frac{1}{2\pi} \fint_B U_1(\underline{r}') \frac{\partial}{\partial n'}\left(\frac{1}{R}\right) dS' \quad , \tag{14}$$

$\underline{r}$ on B, where the bar across the integral sign indicates a Cauchy principal value. If we now write

$$U_1(\underline{r}) = \sum_{j=1}^{3} (\hat{k}.\hat{x}_j)\, U_{1j}(\underline{r}) \tag{15}$$

where (x_1, x_2, x_3) are Cartesian coordinates, the integral equation for $U_{1j}(\underline{r})$ is

$$U_{1j}(\underline{r}) = 2x_j + \frac{1}{2\pi} \fint_B U_{1j}(\underline{r}') \frac{\partial}{\partial n'}\left(\frac{1}{R}\right) dS' \quad . \tag{16}$$

In the far zone $(r \to \infty)$, the Helmholtz representation yields

$$U^s(\underline{r}) \sim \frac{e^{ikr}}{4\pi r} \left\{ -k^2 \int_B \left[\hat{r}.\underline{r}' - U_1(\underline{r}')\right] (\hat{n}'.\hat{r})\, dS' \right.$$

$$\left. + ik^3 \int_B \left[\frac{1}{2}(\hat{r}.\underline{r}')^2 - (\hat{r}.\underline{r}')\, U_1(\underline{r}') + U_2(\underline{r}')\right] (\hat{n}'.\hat{r}) dS' + O(k^4) \right\} \tag{17}$$

where we have used the boundary condition (13), the low frequency expansion (4) and the fact that $U_o(\underline{r}) = 1$. But

$$\int_B (\hat{r}.\underline{r}')(\hat{n}'.\hat{r})\, dS' = V \tag{18}$$

from the divergence theorem, where V is the volume enclosed by B. Also

$$\int_B U_1(\underline{r}')(\hat{n}'.\hat{r})\,dS' = \hat{k}.\overline{\overline{M}}.\hat{r} \qquad (19)$$

where $\overline{\overline{M}}$ is a tensor with elements

$$M_{ij} = \int_B \hat{n}'.\hat{x}_i U_{1j}(\underline{r}')\,dS' \qquad (20)$$

and hence

$$U^s(\underline{r}) \sim \frac{e^{ikr}}{4\pi r} k^2 \left\{ \hat{k}.\overline{\overline{M}}.\hat{r} - V + O(k) \right\} . \qquad (21)$$

As in the case of a soft body, Van Bladel[2] has shown that a knowledge of the potential function appropriate to the leading term is sufficient to specify the next term in the expansion as well. In our notation, the term proportional to ik^3 on the right hand side of (17) is[3]

$$ik^3 \int_B \sum_{j=1}^{3} U_{1j}(\underline{r}') \left\{ (\hat{r}.\hat{x}_j)(\hat{k}.\hat{n}')(\hat{k}.\underline{r}') - (\hat{k}.\hat{x}_j)(\hat{r}.\hat{n}')(\hat{r}.\underline{r}') \right\} dS' \qquad (22)$$

which vanishes in the forward scattering direction, but not for any simple choice of the origin of coordinates. The somewhat more compact form of the k^3 term vis-a-vis Van Bladel's is a consequence of using the total field potential U_1.

From eq. (20) the tensor elements M_{ij} can be written alternatively as

$$M_{ij} = V\delta_{ij} + \int_B \hat{n}.\hat{x}_i \left\{ U_{1j}(\underline{r}) - x_j \right\} dS \qquad (23)$$

where δ_{ij} is the Kronecker delta function, and by application of the divergence theorem,

$$M_{ij} = V\delta_{ij} + \int_{\mathcal{V}} \nabla\left\{U_{1i}(\underline{r}) - x_i\right\} \nabla\left\{U_{1j}(\underline{r}) - x_j\right\} dv \qquad (24)$$

showing that $\overline{\overline{M}}$ is a real symmetric tensor. $\overline{\overline{M}}$ is identical to the magnetic polarizability tensor[4] for a perfectly conducting surface B. It is related to a tensor $\overline{\overline{W}}$ having elements

$$W_{ij} = \int_B \hat{n} \cdot \hat{x}_i \left\{U_{1j}(\underline{r}) - x_j\right\} dS \qquad (25)$$

by the equation

$$\overline{\overline{M}} = V\overline{\overline{I}} + \overline{\overline{W}} \qquad (26)$$

where $\overline{\overline{I}}$ is the identity tensor. $\overline{\overline{W}}$ arises in the study of the irrotational flow of an incompressible inviscid fluid past the rigid surface B, where it is termed the added or virtual mass tensor[5, 6].

The particular advantage of the representation (21) is that $\overline{\overline{M}}$ is a function only of the geometry of B. $\overline{\overline{M}}$ is therefore the counterpart of the electrostatic capacity for a hard body. As shown by Keller et al.[4], an alternative expression for M_{ij} is

$$M_{ij} = \frac{3}{2}\left\{V\delta_{ij} - \int_{\delta V} \hat{x}_i \cdot \nabla\left\{U_{1j}(\underline{r}) - x_j\right\} dS\right\} \qquad (27)$$

where δV is the volume exterior to B but interior to the smallest sphere surrounding B. Thus, if B is a sphere,

$$\overline{\overline{M}} = \frac{3}{2} V\overline{\overline{I}} \quad . \qquad (28)$$

For bodies of more general shape, application of Schwarz's inequality to eq. (24) yields

$$(M_{ii}-V)(M_{jj}-V) \geq M_{ij}^2 \tag{29}$$

for fixed i and j, where repeated suffices do not imply summation. Also,

$$M_{ii} \geq V \tag{30}$$

and other inequalities involving the diagonal elements of the tensor $\overline{\overline{M}}$ are quoted by Payne[6].

There are numerous inequalities satisfied by the capacity, and these can serve to establish upper and lower bounds. One of the most well known is Poincaré's conjecture, since proved by Szegö[7], that of all bodies of given volume the sphere has the least capacity:

$$\frac{C}{4\pi\epsilon} \geq \left(\frac{3V}{4\pi}\right)^{1/3} ; \tag{31}$$

and for all convex bodies at least[8]

$$\frac{C}{4\pi\epsilon} \leq \frac{S^2}{12\pi V} \tag{32}$$

where S is the surface area. All of the inequalities (29) through (32) are optimal in the sense that equality holds for a sphere.

2. ROTATIONALLY SYMMETRIC BODIES

We shall henceforth confine our attention to bodies which are rotationally symmetric about the x_3 axis. It now follows that

$$\begin{aligned} M_{ij} &= 0 \quad , \quad i \neq j \quad , \\ M_{11} &= M_{22} \quad , \end{aligned} \tag{33}$$

so that just two quantities[9], M_{11} and M_{33}, functions only of the geometry, are sufficient to specify the low-frequency (Rayleigh) scattering behavior of a hard body. In terms of these,

$$U^s(\underline{r}) \sim \frac{e^{ikr}}{4\pi r} k^2 \left\{ M_{11}(\hat{k}.\hat{r}) + (M_{33} - M_{11})(\hat{k}.\hat{x}_3)(\hat{r}.\hat{x}_3) + O(k) \right\} . \quad (34)$$

For a soft body,

$$U^s(\underline{r}) \sim \frac{e^{ikr}}{4\pi r} \left(-\frac{C}{\epsilon}\right) \left\{1 + O(k)\right\} \quad (35)$$

showing that the one quantity, C/ϵ, suffices.

Even these three quantities, when normalised appropriately, are relatively slowly varying functions of the geometry. To illustrate this fact, consider a spheroid for which analytical expressions for M_{11}, M_{33} and C/ϵ are available in the form of ratios of Legendre functions of the first and second kinds. By inserting the expressions for these functions, we have

$$M_{11} = \frac{8\pi d^3}{3} \left\{ \frac{1}{2} \log \frac{\xi + 1}{\xi - 1} - \frac{\xi^2 - 2}{\xi(\xi^2 - 1)} \right\}^{-1}$$

$$M_{33} = -\frac{4\pi d^3}{3} \left\{ \frac{1}{2} \log \frac{\xi+1}{\xi-1} - \frac{\xi}{\xi^2-1} \right\}^{-1}$$

$$\frac{C}{\epsilon} = 4\pi d \left\{ \frac{1}{2} \log \frac{\xi+1}{\xi-1} \right\}^{-1}$$

for a prolate spheroid, where ξ $(1 \leq \xi \leq \infty)$ is the radial spheroidal variable and $2d$ is the interfocal distance. The formulae for an oblate spheroid differ

only in having ξ replaced by $i\xi$ and d by $-id$. Moreover,

$$V = \begin{cases} \frac{4\pi}{3} d^3 \xi (\xi^2 - 1) & \text{(prolate)} \\ \frac{4\pi}{3} d^3 \xi (\xi^2 + 1) & \text{(oblate)} \end{cases}$$

and since M_{11} and M_{33} have dimensions $(\text{length})^3$, it is not unnatural to normalise them with respect to V. The resulting normalised quantities are functions of ξ alone and this parameter in turn is directly related to the ratio of the body length ℓ in the axial direction to the body width w in a direction perpendicular thereto. Since C/ϵ has dimensions of length, a possible normalisation factor for this is $4\pi\left(\frac{3V}{4\pi}\right)^{1/3}$. From Poincaré's conjecture, the capacity so normalised has a lower bound of unity and is, in fact, just the (normalised) equivalent radius $\tilde{a}$ of the capacitor, i.e., the ratio of the radius of a sphere having the same capacity as the body to the radius of the sphere having the same volume as B.

For prolate and oblate spheroids, the above normalised quantities are plotted as functions of ℓ/w in Fig. 1. It is seen that M_{11}/V varies from 1 in the disk limit ($\ell/w = 0$), through 1.5 for a sphere ($\ell/w = 1$), to 2 for a long thin prolate spheroid ($\ell/w = \infty$). In contrast, M_{33}/V and $\tilde{a}$ both tend to infinity as $\ell/w \to 0$, but this is due to the vanishing of the normalisation factors rather than to any intrinsic property of M_{33} and C/ϵ. For M_{33} an alternative factor having the appropriate dimensions and producing a variation bounded above and below is the weighted surface integral

$$\tilde{S} = \frac{1}{2}\int \rho \, dS = \pi \int \rho^2 \sqrt{1 + \left(\frac{\partial \rho}{\partial x_3}\right)^2} \, dx_3 \qquad (36)$$

where $\rho = \sqrt{x_1^2 + x_2^2}$ is the transverse radial distance. Clearly, $\tilde{S} \geq V$ with equality in the thin body limit $\left(\frac{\partial \rho}{\partial x_3} = 0\right)$, and in the particular case of the spheroid, $M_{33}/\tilde{S}$ increases from the value $4/\pi$ for a thin disk to a maximum of 1.42 for $\ell/w = 0.27$, and then decreases monotonically through $4/\pi$ for a sphere ($\ell/w = 1$), to 1 for a long thin body ($\ell/w = \infty$).

Since C/ϵ becomes infinite (logarithmically) as $\ell/w \to \infty$, there is no simple geometric quantity with which to normalise this to produce a variation within finite non-zero bounds. Nevertheless, a normalising factor which has been found convenient is one proportional to the average of the length and width of the body. Specifically, we take the factor as

$$L = \pi (\ell + w) \tag{37}$$

and consider the dimensionless quantity $C/\epsilon L$. For a spheroid, this is a monotonic function of ℓ/w, decreasing from $4/\pi$ for a thin disk ($\ell/w = 0$), through 1 for a sphere ($\ell/w = 1$), to 0 for a long thin spheroid ($\ell/w = \infty$). One of the main reasons for choosing the particular normalisation (37) is pointed out in the next Section.

3. NUMERICAL RESULTS

The manner in which the dimensionless quantities M_{11}/V, $M_{33}/\tilde{S}$, and $C/\epsilon L$ vary as functions of the length-to-width ratio ℓ/w has been examined for a variety of rotationally symmetric bodies. Given any particular shape, M_{11}, M_{33} and C/ϵ can be computed by solving the integral equations (6) and (16) satisfied by the respective potential functions. A computer program has been written[3] to solve the equations by the moment method. The only restriction on the body profile is that it be made up of not more than 15 linear or circular arc segments, and for a typical profile, the time required to calculate M_{11}, M_{33} and C/ϵ to an accuracy of better than one-half percent is about 3 seconds on an IBM 360/67 computer.

Data for four generic shapes are shown in Figs. 2 through 4 and the curves for a spheroid are included for comparison. The shapes are:

(i) a rounded cone formed by the intersection of a cone of interior half angle θ and a sphere centered on the apex of the cone. For $\theta \leq 90^{o}$, $\ell/w = \frac{1}{2}$ cosec θ with the value $\theta = 90^{o}$ corresponding to a hemisphere. For $\theta > 90^{o}$, however, the cone is a re-entrant one for which $\ell/w = \frac{1}{2}(1 - \cos\theta)$, and this change in definition of ℓ/w is responsible for the discontinuities in the slope of the plotted curves at $\theta = 90^{o}$.

(ii) ogives ($\ell/w > 1$) and symmetric lenses ($\ell/w < 1$) obtained, respectively, by rotating an arc of a circle about its chord, and by rotating two identical arcs about their common bisector. The transitional shape is a sphere.

(iii) a right circular cylinder of length ℓ and radius $w/2$.

(iv) a spherically-capped cylinder. For $\ell/w > 1$ the cylinder is a right circular one of length $\ell - w$ and radius $w/2$ capped by two hemispheres of radius $w/2$, thereby forming a 'cigar'. For $\ell/w < 1$ the caps are placed on the longitudinal sides, producing a body whose profile is a rectangle of length ℓ and width $w - \ell$ with semi circles of radius $\ell/2$ top and bottom. The transitional shape, when $\ell/w = 1$, is again a sphere.

When Figs. 2 through 4 are examined, the impression gained is that the behavior of the three normalised quantities as functions of ℓ/w is very similar for all of the bodies. Thus, in Fig. 2, the greatest departure[10] from the corresponding value for a spheroid is less than 10 percent, suggesting that as regards M_{11}/V the spheroid provides an accurate means of estimating the variation as a function of ℓ/w. This is true even for an asymmetric body (the rounded cone), including cases where the body is a re-entrant one, e.g. the cone with half-angle $\theta > 90^{o}$. Of course, V and ℓ/w are not sufficient to uniquely specify a body, and M_{11}/V can display greater departures from the spheroidal norm for shapes other and more complicated than those we have examined. Consider, for example, two hemispheres face to face which may

or may not be joined by a wire of infinitesimal thickness. For this body V is constant regardless of $\ell/_w$ and as the separation between the hemispheres is increased from zero ($\ell/_w = 1$), $M_{11}/_V$ decreases from the value 1.50 appropriate to a sphere, becoming 1.46 for $\ell/_w = 1.1$, 1.40 for $\ell/_w = 1.5$ and 1.38 for $\ell/_w = 2.5$. Ultimately, as $\ell/_w \to \infty$, $M_{11}/_V \to 1.37$, the value for a hemisphere in isolation.

Similar conclusions apply to $M_{33}/\tilde{S}$, where the normalisation $\tilde{S}$ confines the maximum variation within finite non-zero bounds for at least the class of shapes considered here. Once again the spheroid provides a reasonable basis for estimation even for asymmetric bodies.

For $C/_\epsilon$, the normalisation with respect to L produces an upper limit on the variation. Indeed, since[8]

$$\frac{C}{4\pi\epsilon} \leq D$$

where D is the maximum separation of any two points on the surface, and

$$D < \ell + w \ ,$$

it follows that

$$\frac{C}{\epsilon L} < 2 \ ,$$

but because of the logarithmic decrease in the capacity of any body as $\ell/_w \to \infty$, $C/_{\epsilon L}$ approaches zero in the limit. There is also more spread about the corresponding spheroid value than was the case in Figs. 2 and 3 and this could have been reduced by choosing a normalising factor based on either the surface area of the body or its profile length. Such normalisations have a major drawback, however. For a body which is re-entrant or has an aperture, the capacity is continuous even in the limit as the aperture size is decreased to zero. Since the surface area and profile length are discontinuous in this limit, either leads

to a discontinuity in the normalised capacity, and the disadvantage of using the volume (which is continuous) is evident from Fig. 1.

4. CONCLUSIONS

In low frequency (Rayleigh) scattering by acoustically hard bodies there are considerable advantages in introducing the concept of the magnetic polarizability tensor $\overline{\overline{M}}$ which is a function only of the geometry of the body. In the particular case of rotational symmetry the tensor naturally diagonalises and just two of its elements are independent. A knowledge of the elements M_{11} and M_{33} is then sufficient to specify the entire low frequency scattering behavior in just the same way as the electrostatic capacity C/ϵ specifies the low frequency scattering by an acoustically soft body. Even these quantities are subject to known constraints in terms of the geometrical properties of the body.

We have shown that for a variety of shapes of interest in acoustic scattering, appropriate normalisation of M_{11}, M_{33} and C/ϵ reduces their variation to such an extent that the spheroid, prolate and oblate, can serve as a means of estimating these quantities to an accuracy sufficient for many practical objectives. Alternatively, M_{11}, M_{33} and C/ϵ can be calculated exactly using an efficient computer program constructed for this purpose.

REFERENCES

1 hereinafter referred to as a field.

2 J. Van Bladel, J. Acoust. Soc. Amer. 44, 1069-1073 (1968).

3 T.B.A. Senior and D.J. Ahlgren, "The Numerical Solution of Low Frequency Scattering Problems," The University of Michigan Radiation Laboratory Report No. 013630-9-T (February 1972).

4 J.B. Keller, R.E. Kleinman and T.B.A. Senior, J. Inst. Maths. Applics., 9 (1972): to be published.

5 M. Schiffer and G. Szegö, Trans. Amer. Math. Soc., 67, 130-205 (1949).

6 L.E. Payne, SIAM Rev., 9, 453-488 (1967).

7 G. Szegö, Math. Z., 31, 583-593 (1930).

8 G. Szegö, Math. Z., 33, 419-425 (1931).

9 It is of interest to note that for all rotationally symmetric bodies $M_{33} = \frac{1}{2} P_{11}$ where $\overline{\overline{P}}$ is the electric polarizability tensor.

10 For all rotationally symmetric convex shapes, it has been conjectured[11] that $M_{11}/_{V} \leq 2$, and proved[11] that $M_{11}/_{V}$ does have a finite upper bound, in contrast to $M_{33}/_{V}$.

11 R.E. Kleinman and T.B.A. Senior, Radio Sci., 7, (1972): to be published.

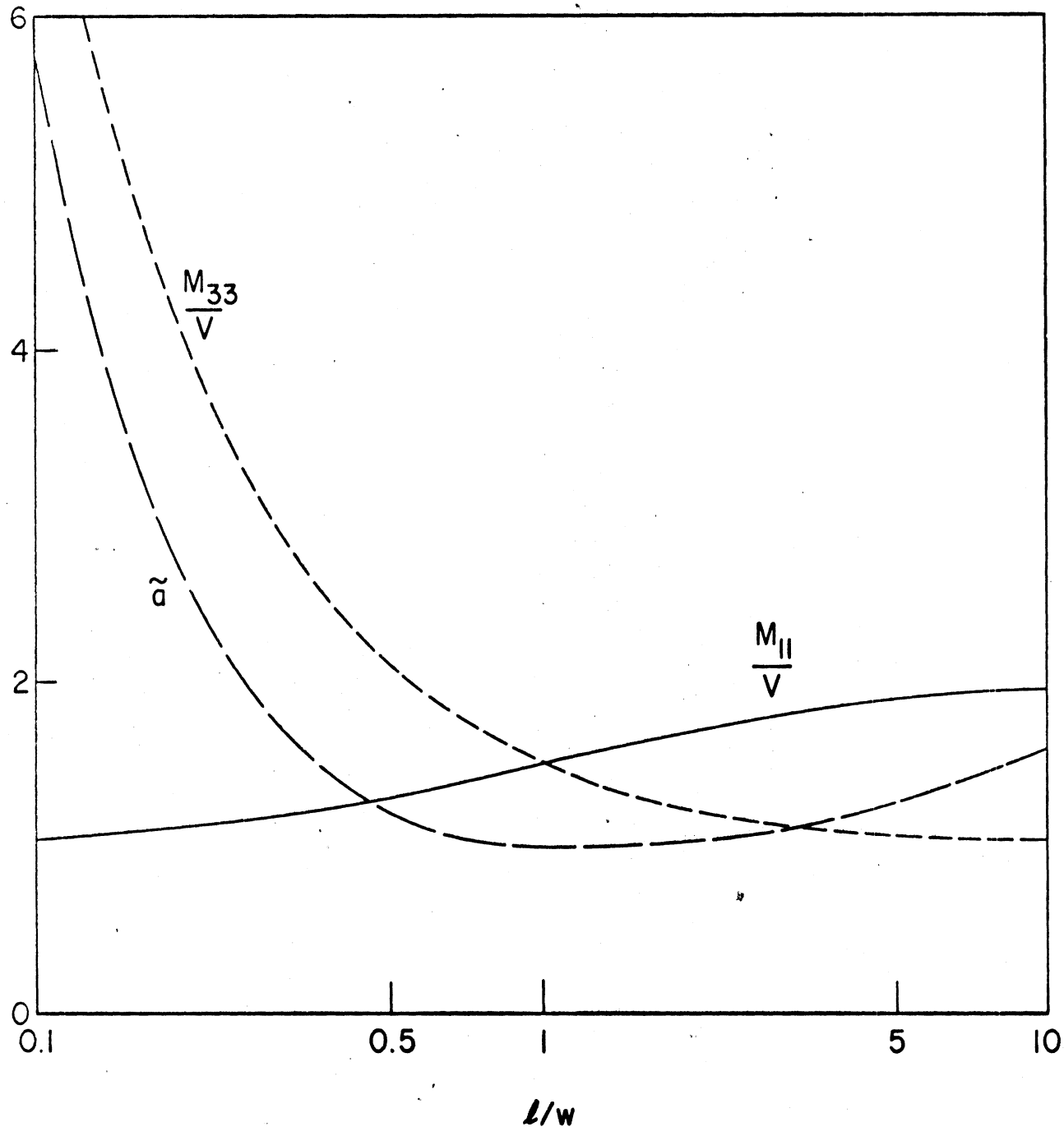

Fig. 1.

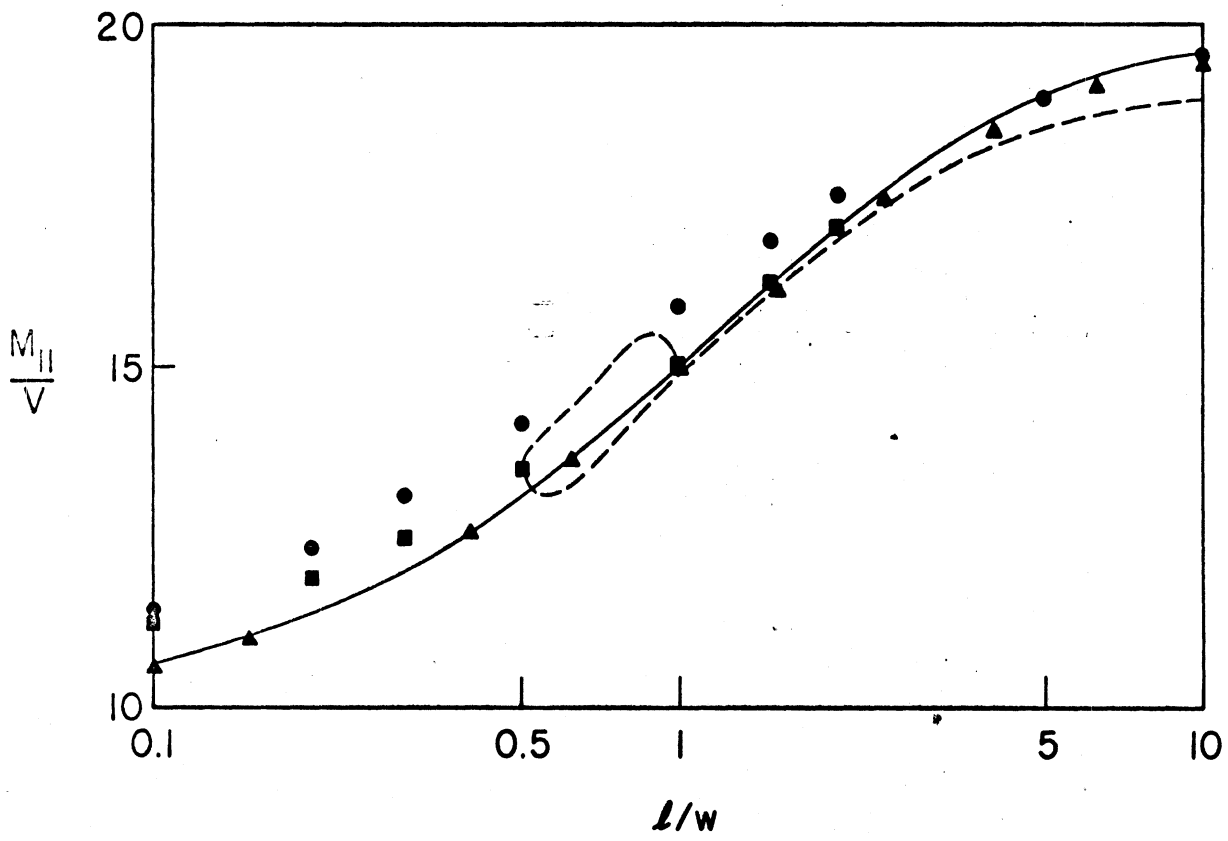

Fig. 2.

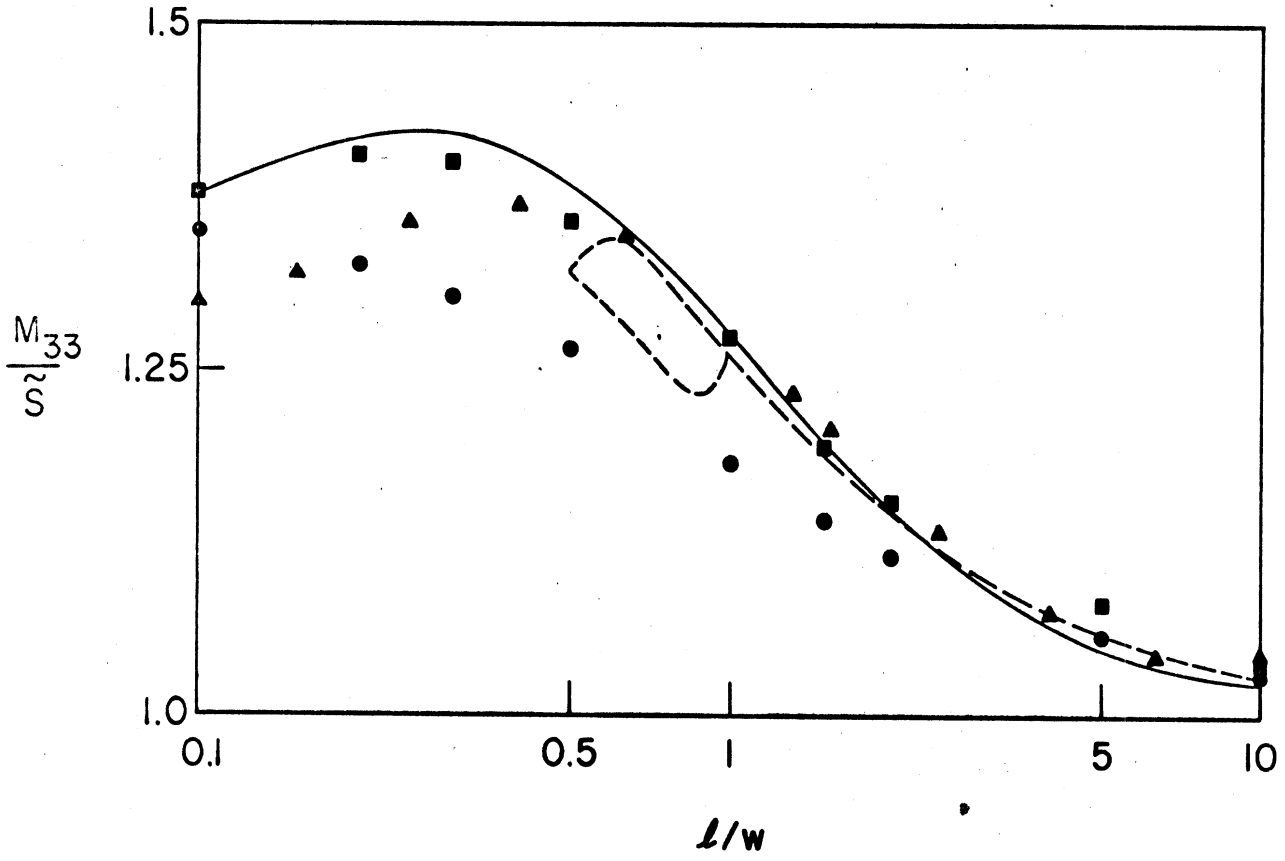

Fig. 3.

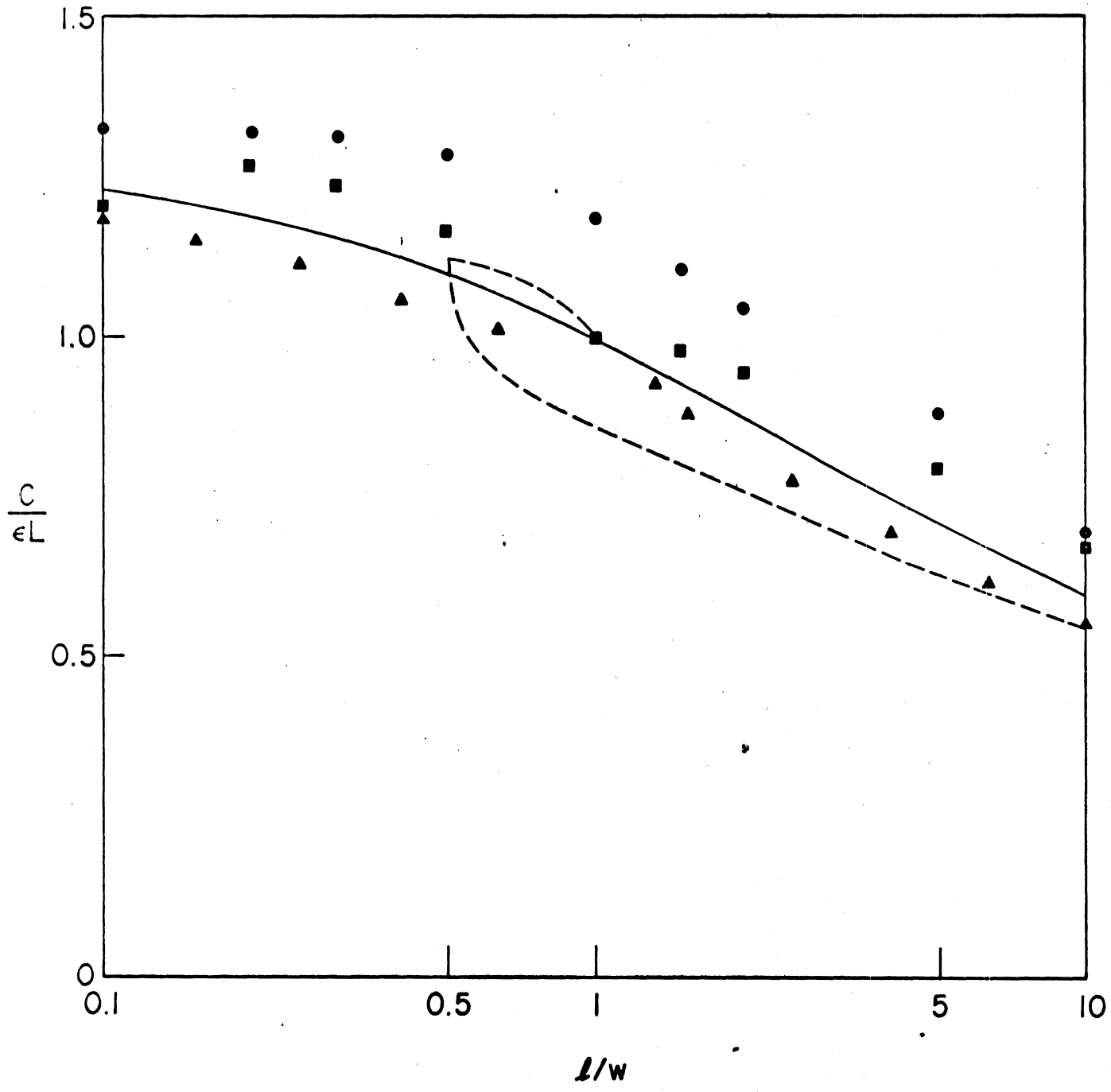

Fig. 4

Legends for Figures

Fig. 1: $\frac{M_{11}}{V}, \frac{M_{33}}{V}$ and $\tilde{a}$ for oblate and prolate spheroids.

Fig. 2: $\frac{M_{11}}{V}$ versus $\frac{\ell}{w}$ for spheroids (——), rounded cones (---), ogives and lenses (▲▲), right circular cylinders (● ●) and capped cylinders (■■).

Fig. 3: $\frac{M_{33}}{\tilde{S}}$ versus $\frac{\ell}{w}$: the symbols are as in Fig. 2.

Fig. 4: $\frac{C}{\epsilon L}$ versus $\frac{\ell}{w}$: the symbols are as in Fig. 2.